

Accurate module performance characterisation using novel outdoor matrix methods

Steve Ransome and Juergen Sutterlueti

Steve Ransome Consulting Ltd, #99 KT 26AF, Kingston upon Thames, UK. steve@steveransome.com

Abstract—Indoor PV module characterization is performed with a matrix of 6-23 irradiance and module temperature points (G,T). Separate angle of incidence and spectral measurements are needed. Reducing the number of matrix points would lower measurement costs but may reduce modelling accuracy.

Outdoor PV module characterization uses frequent measurements (IV or Pmp) under actual weather conditions which include angle of incidence, diffuse fraction, and spectral effects. Measuring every minute can give ~260k records/year. These need good data sanitizing and filtering for accurate understanding.

This paper shows novel methods to analyse matrix data much better than 6-23 points to generate the following :-

- 1) Outdoor matrices (~100 points) for PR_{DC}, Voc, Isc etc.
- 2) Better modelling accuracy and performance checking.
- 3) Degradation rates and causes (e.g. %Voc fall/year).
- 4) Quantified technology differences e.g. cSi vs. Thin Film.
- 5) Pmp values at different conditions STC, LIC, PTC etc.
- 6) Temperature coefficients e.g. gamma(Pmp), dRoc/dTmod.
- 7) Problem finding such as “lower Rshunt than expected”.
- 8) Comparison of outdoor with indoor reference IV curves.

A mechanistic fitting approach is used for the modelling, 6 parameters are sufficient to model c-Si and HIT well. Residual errors of the matrix points can show if extra mechanistic coefficients need to be added for even closer modelling fits. An enhanced model with meaningful, independent coefficients has been used for any non-linear modules e.g. some thin films where gamma (dPR_{DC}/dTmod) can vary a little with Tmod and/or Irradiance.

Much of this improved matrix analysis can be performed with only (Imp and Vmp) or Pmp values.

The data analysed is from many different PV technologies (>15 modules both cSi and Thin Film) which have been measured from ~2011-2021+ at Gantner Instruments’ OTF in Tempe AZ

Keywords— energy, modeling, photovoltaic systems, power, simulation, degradation

I. INTRODUCTION

A PV module that behaves linearly can be fitted just by sums of functions of irradiance, temperature and windspeed independently such as :

$$PR_{DC} = f(G) + f(T) \quad [\text{no } f(G,T) \text{ non-linear terms}]$$

DC Performance ratio is defined as :-

$$PR_{DC} = \text{measured_P}_{MP} / \text{reference_P}_{MP} / G_{TI_suns} \quad (1)$$

The performance of a module vs. irradiance and module temperature is usually shown on datasheets and in simulation programs such as PVSYST in the format shown in Fig.1.

Each temperature line has a logarithmic fall due to R_{SHUNT} and V_{OC} at low light and a linear drop due to R_{SERIES} at high light. A linear module has a constant vertical separation between the temperature lines (gamma %/K).

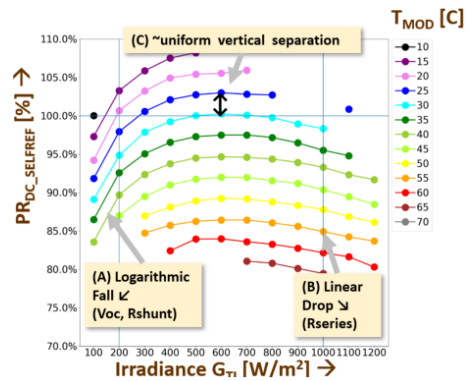


Fig. 1. Datasheet style representation of the performance of a linear PV module.

A. Indoor matrix characterisation

Indoor characterization of PV Modules (according to IEC 61853) is done by measuring performance at up to 23 plane of array irradiance G and module temperature T_{MOD} points (G, T) as shown in Fig. 2. Separate measurements are needed for the spectral and angle of incidence dependencies [1,2,3]. The standard IEC 61853 (G, T) values had been chosen to cover the ranges experienced in most climates (e.g. 100-1100W/m², 15-75C).

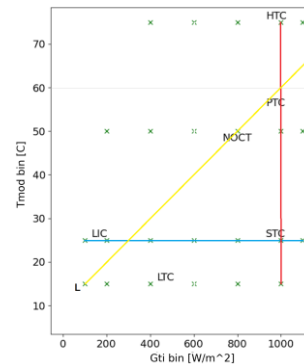


Fig. 2 IEC Matrix measurement conditions vs. Tmodule and irradiance Gti. Standard IEC 61853 matrix conditions marked “X”.

B. Matrix characterisation from outdoor measurements

Outdoor measurements are often taken frequently (~1 minute) with irradiance values 0 to ~1200W/m² and module temperatures ~ -10 to +70C (both depending on climate). Diffuse fractions DF (= 1 - Beam_horizontal / Global_horizontal) usually vary from ~0.1 to ~0.9, angles of incidence may vary from 0° to > 90° (i.e. the sun is behind the array) and spectra from <AM1.5 to >AM10 (which depend on latitude, season, time of day and atmospheric conditions).

Measurement scatter occurs after cloud events. These should be filtered out for best analysis, particularly as module temperatures may take up to 15 minutes to stabilize after transient weather changes.

C. Outdoor measurement setup used in this work

High quality meteorological and IV measurements have been taken every minute by Gantner Instruments' OTF in Tempe Arizona [ref] for more than 10 years with more than 30 modules of all common technologies c-Si, HIT, CdTe, CI(G)S, aSi:aSi, aSi:ucSi etc. Fig. 3 shows a view of the Gantner Instruments OTF used in this work.



Fig. 3. Gantner OTF at Tempe AZ.

Details of the OTF measurements setup are given below :

PV Modules Measurements: Fixed and 2D track; IV curve every minute, all environmental sensors, spectral parameters
PV Module Power : up to 500W/800W
High quality digitalization, current accuracy 0.1% FS, voltage: 0.05% FS
Scalable system (4 .. 48 channels) with raw data access : Local or cloud-based data streaming
Derived parameters using Loss Factors and Mechanistic Performance Models
Integrated Python Jupyter Lab for direct analysis and automatic reporting
Continuous measurements in Arizona since 2010; Other sites available around the world

GI OTF MEASUREMENTS

Name	Description	Units
GH	Global Horizontal Irradiance	kW/m ²
DH	Diffuse Horizontal Irradiance	kW/m ²
BN	Beam Normal Irradiance	kW/m ²
Gi	Global Inclined Irradiance (Pyranometers and c-Si ref cells)	kW/m ²
T _{AMB}	Ambient Temperature	C
T _{MOD}	Back of Module Temperatures	C
WS	Wind Speed	ms ⁻¹
WD	Wind Direction	°
RH	Relative Humidity	%
G(λ)	Spectral Irradiance G(350– 1050nm)	W/m ² /nm

II. IMPROVED OUTDOOR MATRIX ANALYSIS

Fig 4 shows analysis of raw outdoor measurements to sanitised average PR_{DC} matrices of ~100 bins. Colour coding (blue best, red worst) is for PR_{DC} for a typical cSi module.

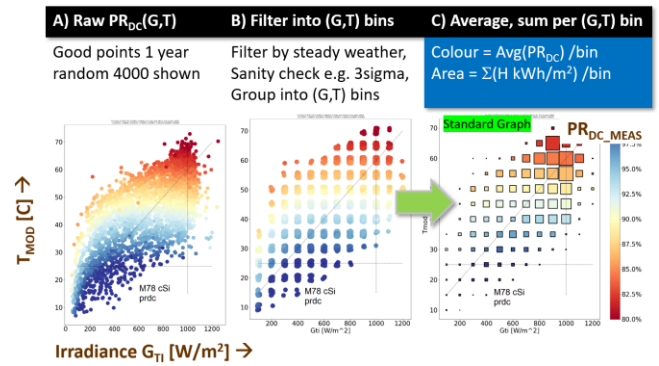


Fig. 4. Averaged PR_{DC} / bin from good quality measurements Typical cSi, Gantner Instruments, Tempe AZ

a) Raw PR_{DC}(G,T) measurements

Approximately 4000 random measurements (1/hour) for a year are shown in fig. 4A. PR_{DC} falls (redder) with increasing temperature(↑) and at both lowest(←) and highest irradiance(→)

b) Filtered PR_{DC} data into (G,T) bins

To reduce the number of measured points to be analysed and improve modelling, only data under stable weather conditions was selected (i.e. almost constant (G,T) values for a few consecutive minutes) and points within 3 sigma [4,5].

With well measured, non-scattered data the filtered points within each bin are mostly uniform (constant colour) as in the fig. 4B.

c) Averaged, Summed per (G,T) bin

The averaged PR_{DC} per (G,T) bin is shown in Fig. 4C. The areas of the squares are proportional to the insolation H_{Ti} (~kWh/m²/year) in each bin, larger squares are therefore more important in fitting and generating energy yield. In this location (AZ) the maximum insulations are seen to be (G≥900W/m², T≥55C). This format is referred to as “the standard graph” as it is used throughout the work.

A. Comparing PR_{DC} per matrix bin by technology

Fig. 5 plots standard graph for four typical modules (M78 cSi, M31 HIT, M72 CdTe and M81 CIGS). All modules are

seen to have a smooth and monotonic variation in PR_{DC} shown by the PR_{DC} colours indicating good measurements and binning.

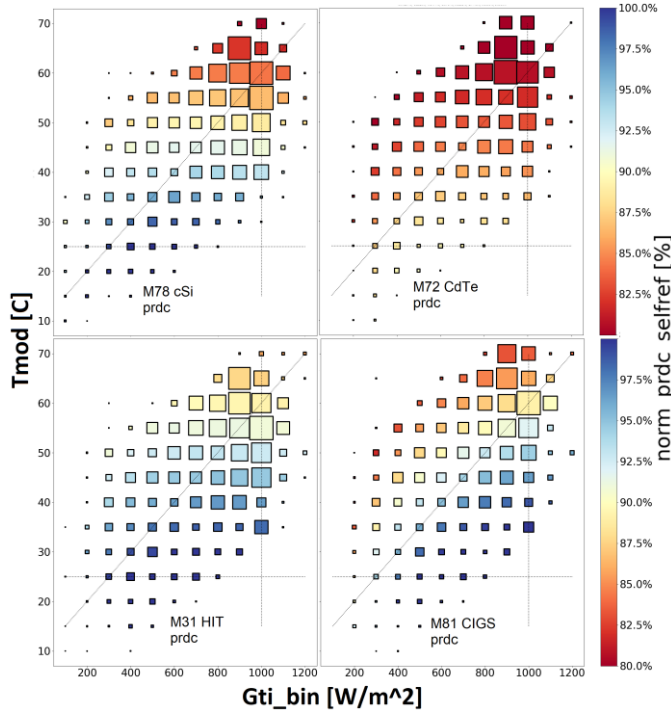


Fig. 5. Averaged $PR_{DC_SELFREF}(G,T)$ vs. bin, Gantner Instruments, Tempe AZ.

III. GENERATING NORMAL DATASHEET FORMAT GRAPHS

Fig. 6. demonstrates replotting standard matrix data in the format usually used on datasheets. Each horizontal row of matrix points (left) has the data of PR_{DC} (colour) vs. irradiance (x) at a constant temperature (y). Replotting each temperature as a coloured line as PR_{DC} (y) vs. irradiance (x) gives the graph on the right. The vertical separation ($dPR_{DC}/dT_{MOD} = \text{gamma}$) seems constant for this module.

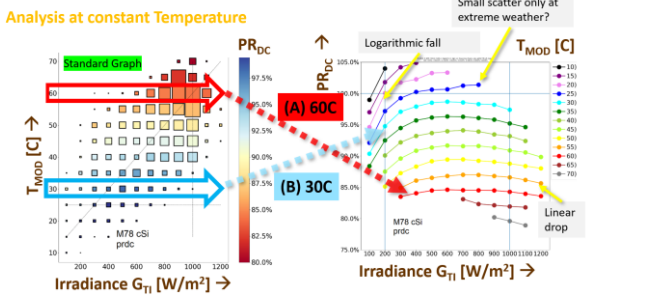


Fig. 6. Standard graph data to datasheet format graphs for typical cSi module. Gantner Instruments, Tempe AZ.

Fig. 7 compares the graphs for the four example modules. M78 cSi, M31 HIT and M72 CdTe look quite linear over the matrix area (although extreme weather points may have a little scatter).

CIGS module M81 has a different shape with rising PR_{DC} at high G and larger gamma separation \uparrow at high temperatures \downarrow which indicates a little non-linearity.

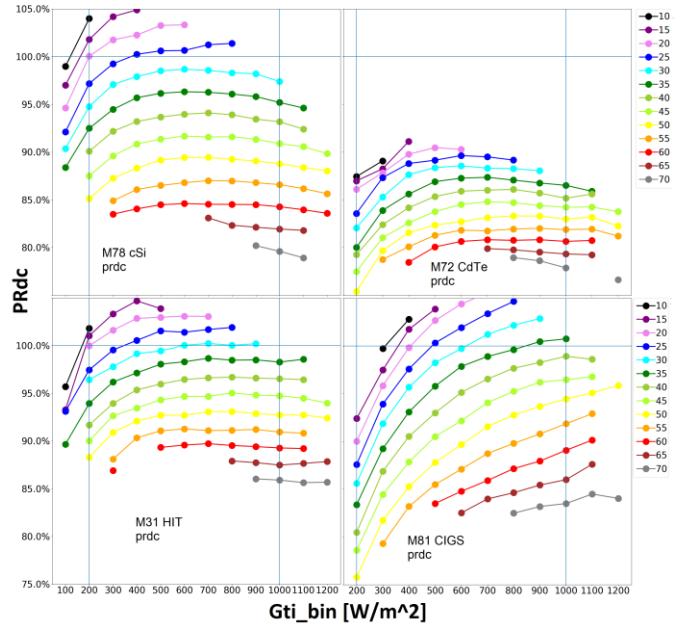


Fig. 7. $PR_{DC_SELFREF}$ vs. G_{Ti} (x axis), coloured lines show module temperature [C] for four typical modules Gantner Instruments, Tempe AZ.

IV. TEMPERATURE COEFFICIENT HEATMAPS

The power temperature coefficient $\gamma(G,T)$ is given by equation (1).

$$\gamma(G, T) = \Delta PR_{DC}(G, T) / \Delta T_{MOD} \quad [\% / K] \quad (2)$$

Fig. 8 illustrates how to analyse the standard graph points vertically to find the slopes of $PR_{DC}(G, T)$ by $T_{MOD}(x)$ for each insolation bin (coloured lines).

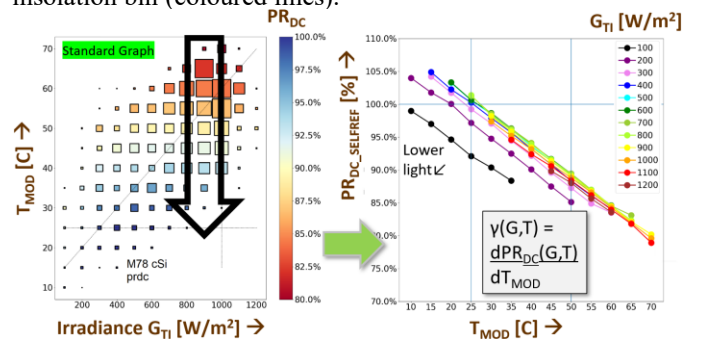


Fig. 8. Standard graph data (left) to $PR_{DC}(y)$ vs. $T_{MOD}(x)$, typical cSi module. Gantner Instruments, Tempe AZ

V. DERIVING GAMMA HEATMAPS

Fig. 9 replots the $\gamma(G,T)$ as a heat map over the 100 (G,T) bins. They are all quite smooth indicating well measured data with little scatter and noise. Nominal datasheet values are given. Colour bars $-0.02\%/K$ dark blue to $-0.68\%/K$ dark red. The cSi and HIT modules $\gamma(G,T)$ look to be almost constant over all irradiances and temperatures with the HIT having a lower measured value as expected from the nominal datasheet value. CdTe is seen to have a slightly worse γ at low temperature and irradiance (pale yellow vs. blue). CIGS modules have γ value is worse at higher irradiance and temperature (dark red) than at low irradiance and temperature

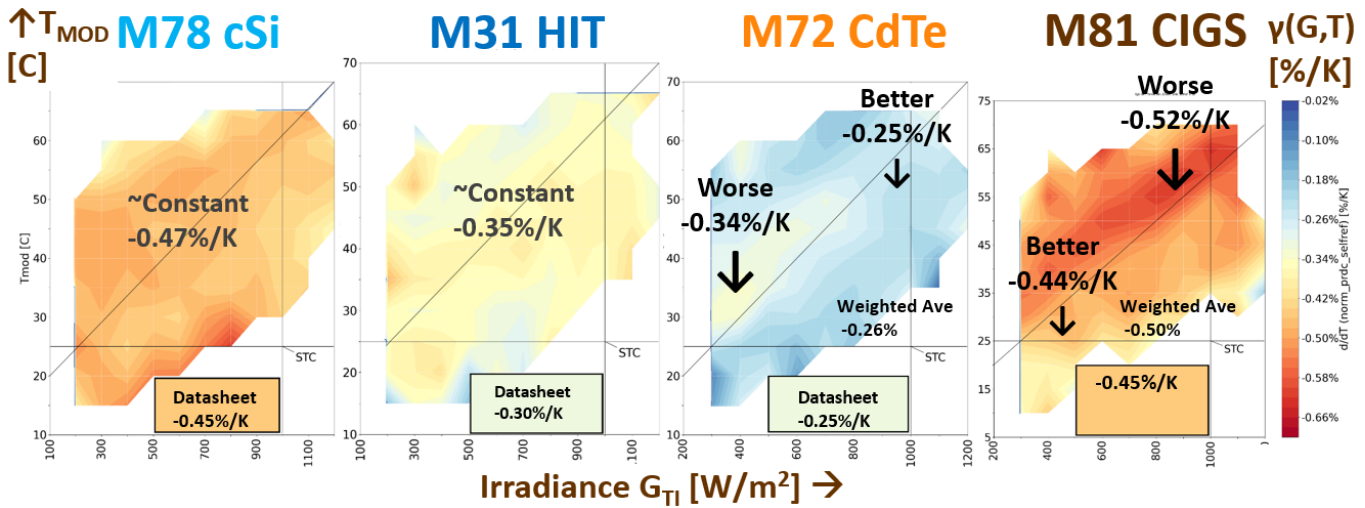


Fig. 9. Gamma heatmaps for four modules. Gantner Instruments, Tempe AZ.

VI. PRDC PERFORMANCE MODELLING AND FITTING

A mechanistic model `mpm_6` which has six normalised coefficients has been proven to model linear modules well such as c-Si and HIT and most CdTe.

```
# PYTHON MPM 6 MODEL
# c_1 .. c_6 : normalised coefficients
# gti = plane of array irradiance [kW/m^2]
# tmod = module temperature [C]
# ws = wind speed [ms^-1]
T_STC = 25 #

def mpm_6(gti,tmod,ws, c_1,c_2,c_3,c_4,c_5,c_6):
# mechanistic performance returns PRdc value
    return (
        c_1 + # overall efficiency
        c_2 * (tmod - T_STC) + # temp coeff
        c_3 * np.log10(gti) + # low light Voc, Rsh
        c_4 * gti + # high light Rs
        c_5 * ws + # windspeed
        c_6 / gti # Rsh (optional, < 0)
    )
```

Several of the modules at Tempe have also had their derived average βV_{OC} and γP_{MP} coefficients checked against datasheet

values as given in Table III (presently the procedure averages out any non-linearities seen in fig. 7 to give one value).

The methodology can also calculate averaged temperature coefficients of R_{SC} ($\sim R_{SHUNT}$) and R_{OC} (which is dominated by R_{SERIES}).

Without spectral/soiling correction this method can't yet give alpha coefficients as accurately (as spectrum and temperature correlate, clear skies tend to be hotter and bluer).

The calculated beta Voc matches the datasheet values to within $\pm 0.02\%$, for the cSi modules the gamma is $\pm 0.03\%$ for most but the CIGS devices don't yet fit well due probably due to the small non-linear effects which will be worked on further.

Typical `mpm_6` fit results are shown in Table III for many module technologies. The `c_2` coefficient is an averaged gamma over all data points, with better lower values for CdTe and HIT than other cSi.

The nominal value STC is calculated by $STC = c_1 + c_4 + c_6$ (obtained by substituting $gti=1$ and $tmod=25$ into the `mpm_6` formula). LIC is an equivalent calculation but with $gti=0.2$.

TABLE III : DATASHEET, CALCULATED AND DIFFERENCE TEMPERATURE COEFFICIENTS, MPM6 FIT COEFFICIENTS PER MODULE

tech-nology	mod id	alphaIsc			betaVoc			gamma Pmp			MPM coefficients						STC	LIC	LIC/STC
		manuf	calc	diff	manuf	calc	diff	manuf	calc	diff	c_1	c_2	c_3	c_4	c_5	c_6			
CIGS	71	0.01%	-0.02%	-0.02%	-0.30%	-0.30%	0.00%	-0.31%	-0.44%	-0.13%	115.7%	-0.44%	22.7%	7.8%	-0.1%	0.8%	107.2%	94.5%	88.2%
CIS/CIGS	81	-0.03%	0.01%	-0.07%	-0.36%	-0.37%	-0.01%	-0.44%	-0.50%	-0.06%	110.6%	-0.50%	14.2%	1.5%	0.0%	2.5%	106.6%	87.8%	82.4%
CdTe	11	0.04%	0.01%	0.08%	-0.25%	-0.23%	0.02%	-0.25%	-0.19%	0.06%	95.9%	-0.19%	6.1%	1.9%	0.1%	2.7%	81.3%	75.9%	93.4%
CdTe	72	0.04%	0.00%	-0.02%	-0.27%	-0.26%	0.01%	-0.25%	-0.26%	-0.01%	96.4%	-0.26%	0.8%	4.0%	0.0%	2.7%	89.7%	82.5%	92.0%
c-Si	12	0.03%	-0.01%	-0.07%	-0.34%	-0.34%	0.00%	-0.48%	-0.48%	0.00%	111.6%	-0.48%	19.3%	1.2%	0.0%	0.0%	100.4%	95.9%	95.5%
c-Si	78	0.05%	0.02%	-0.07%	-0.35%	-0.33%	0.02%	-0.45%	-0.47%	-0.02%	109.6%	-0.47%	12.5%	3.7%	0.0%	0.4%	100.5%	97.2%	96.7%
c-Si	83	0.05%	0.01%	-0.08%	-0.32%	-0.32%	0.00%	-0.43%	-0.46%	-0.03%	105.4%	-0.46%	15.0%	9.3%	0.0%	-0.1%	96.0%	92.7%	96.5%
c-Si	85	0.05%	0.04%	-0.08%	-0.32%	-0.30%	0.02%	-0.42%	-0.42%	0.00%	104.0%	-0.42%	10.0%	8.6%	0.0%	0.4%	95.0%	93.3%	98.2%
HIT	31	0.03%	-0.02%	-0.03%	-0.25%	-0.26%	-0.02%	-0.30%	-0.35%	-0.05%	109.5%	-0.35%	11.5%	7.3%	0.0%	-0.5%	101.7%	97.4%	95.8%

A. Residual fit error matrix maps

Fig. 10 shows residual fit error matrix plots using the `mpm_6` function. Pale yellow indicates a good fit, blue indicates over performance and orange underperformance. Checking residual errors of the matrix points can show if any extra mechanistic coefficients need to be added for closer modelling fits if any modules have non linear behaviour such as some CdTe and CIGS. The limits shown are -2.0 to $+2.0\%$ / bin but as can be seen the cSi, HIT and CdTe modules have fit errors less than $\pm 0.25\%$ for almost all bins. (This proves the good accuracy of the `MPM_6` fit method for these technologies).

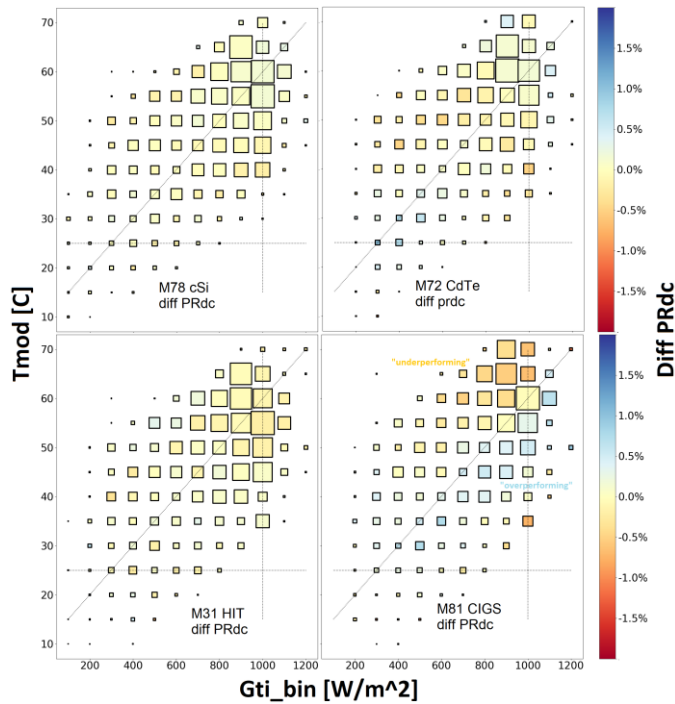


Fig. 10. Residual errors of PR_{DC} vs G_{Ti} and T_{MOD} bins for four typical modules. Gantner Instruments, Tempe AZ.

The CIGS module has small monotonically varying errors (highlighted). At low irradiance and temperature the module is fitted well (pale yellow), at high irradiance the module underperforms at higher temperatures (orange) and overperforms at lower temperatures (blue). The magnitude and signs of these discrepancies can be used to determine what is causing it and define any additional fit coefficients needing to be added to the `mpm_6` model. The residual fit errors from different technologies might not be of similar shapes and causes and different coefficients may be needed for various technologies for ultimate fit accuracy.

VII. IDENTIFYING AND QUANTIFYING ANY NON LINEAR BEHAVIOUR

Six Loss Factors Model parameters can all be measured and analysed. The LFM models PR_{DC} performance as the product of the normalised loss coefficients as illustrated in fig. 11.

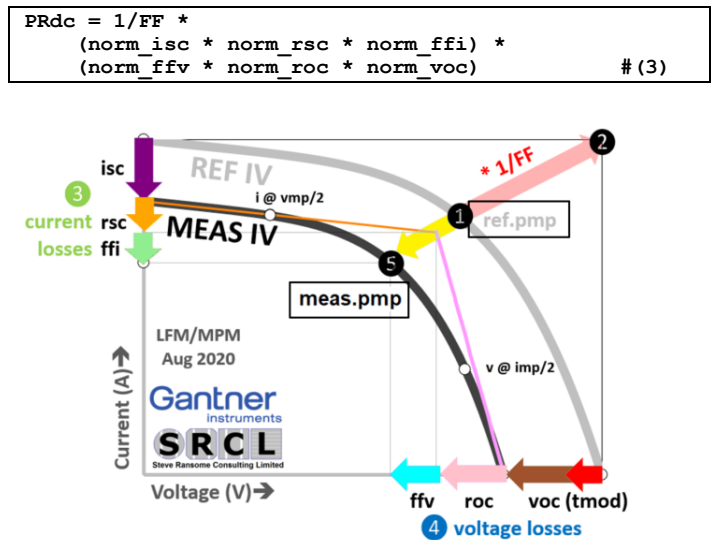


Fig. 11. Loss Factors model coefficients.

Three parameters (`norm_isc`, `norm_ffi`, and `norm_ffv`) seem to be almost constant for these modules so the fit errors for only `norm_rsc`, `norm_roc` and `norm_voc` are given in fig 12. As the PR_{DC} is the product of the six LFM parameters matrices, similar discrepancy shapes for a parameter to PR_{DC} indicates they are causing its behaviour. It can be seen that the `norm_rsc` and `norm_voc` residual fits have good low discrepancies, indicating they do not cause the PR_{DC} . A similar shape/colours can be seen with `norm_roc` indicating it is the main cause.

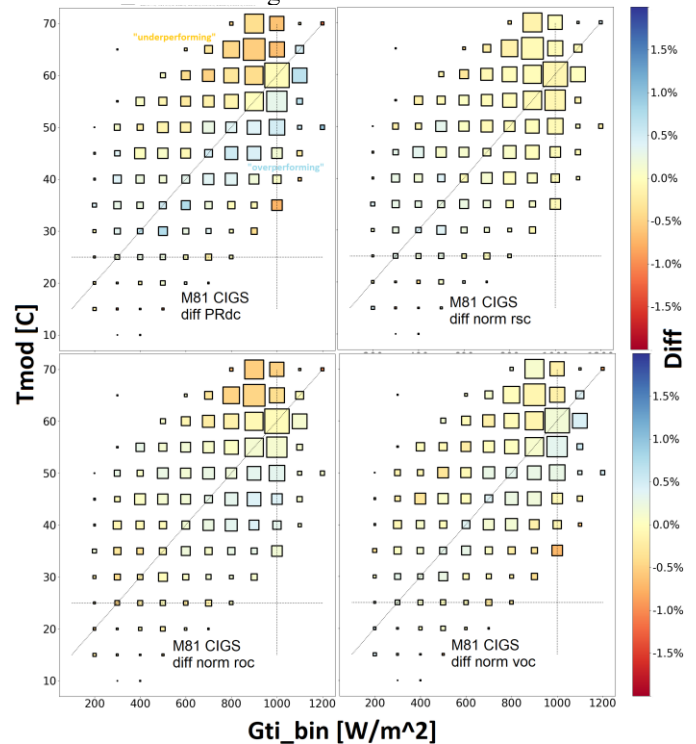


Fig.12. Residual errors of M81 CIGS for PR_{DC} , `norm_rsc`, `norm_roc` and `norm_voc`. Gantner Instruments, Tempe AZ.

A simple method (to be published) is used to extract the intrinsic series Resistance `meas_rs` from the LFM parameter

norm_roc. Figure 13 plots the meas_rs behaviour of cSi (left) which is very similar to the behaviour of the HIT and the CdTe indicating almost temperature independency. The CIGS looks very different with a very temperature dependent meas_rs at high irradiance. The physical and electrical reasons aren't yet known but the factor causes the non linear PR_{DC} behaviour

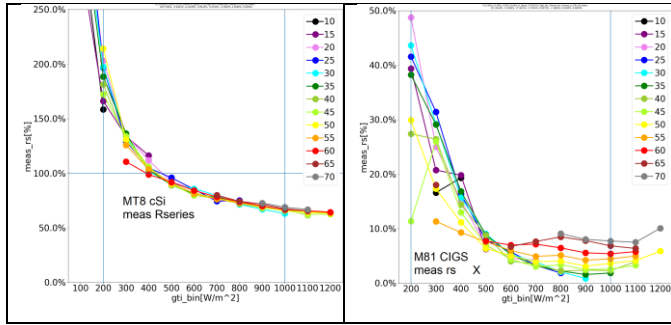


Fig.13. Extracted meas_rseries vs. irradiance (x) and Tmod (coloured lines) for cSi M78 (left) vs. M81 CIGS (right). Gantner Instruments, Tempe AZ.

At least three types of small (<±0.5%?) non-linear perturbations have been found and are given fig. 14. Pattern matching of the discrepancies for the LFM coefficients will enable the effects to be understood and technology dependent correction parameters added to the usual linear model when highest accuracy is needed. Probable causes for the non linearity are shown on the graphs. These effects will be investigated further.

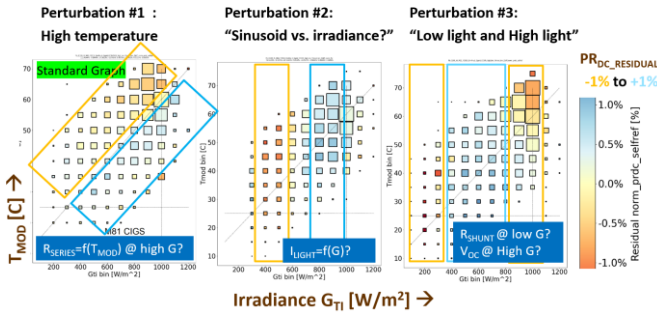


Fig.14. Three different types of non linear perturbations found with probable causes shown. Gantner Instruments, Tempe AZ

VIII. METEOROLOGICAL DATA ANALYSIS

The OTF meteorological sensors are very accurate and provide good data so they have also been analysed. Some examples are given here.

A. Apparent irradiance Ref_cell vs. Pyranometer

The Irradiance ratio reported by a cSi reference cell divided by the Irradiance from a pyranometer are shown in fig. 15 against beam fraction(→) and angle of incidence(↑).

$$G_{REFCELL_PYR} = \frac{G_{REF_CELL}}{G_{PYRANOMETER}} \quad [\%] \quad (4)$$

(A) Lower angles of incidence <50. G_{REFCELL_PYR} is quite flat around 99%,

(B) Higher angles of incidence the value falls as the angular dependence of a reference cell falls more quickly than a pyranometer,

(C) Clear sky (high beam fractions) with high AOI the value ratio falls most rapidly indicating the discrepancy is highest at clear skies with grazing incidence.

The smoothness of the graph indicates the quality of the measurements and the worse reflectivity vs. angle of incidence that the ref cell has vs. the pyranometer.

Redundancy checks can be made with all the irradiance sensors using data such as this to show if any sensors are drifting, soiled or are faulty.

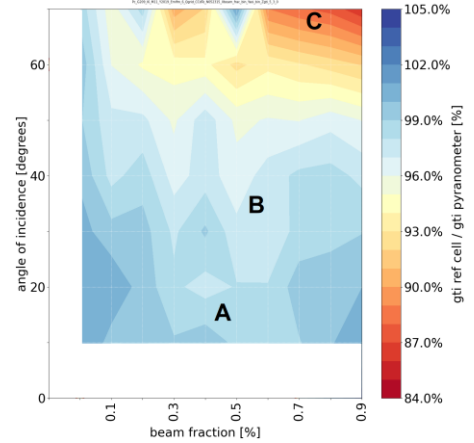


Fig. 15. G_{REF_CELL_PYR} vs. beam_fraction and aoi. Gantner Instruments, Tempe AZ

B. Apparent spectral irradiance of an unfiltered ref cell /KG_3 ref cell vs. blue fraction

Fig. 16 shows the G_{TI} irradiance ratio (coloured dots) measured by an unfiltered reference cell / KG3 reference cell vs. clearness index kTh (y) and blue fraction (x) where BF = G(350..650nm)/G(350..1050nm). The data can be summarised as follows :

(A) Clear (high kTh) mornings and evenings (low sun) will be red rich.

(C) Dull (low kTh), cloud filtering results in blue rich.

(B) At other times there can be a wide variety of clearness index (y), the G_{TI} ratio will depend on the blue fraction giving vertical bars of constant colour as are seen here.

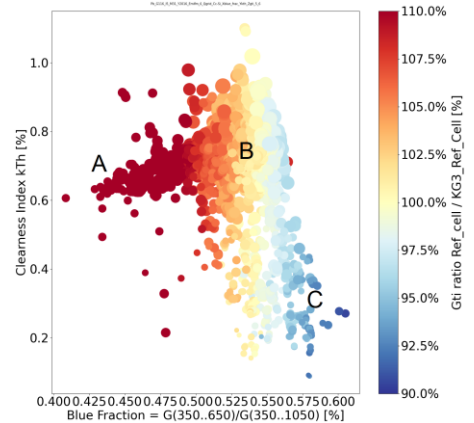
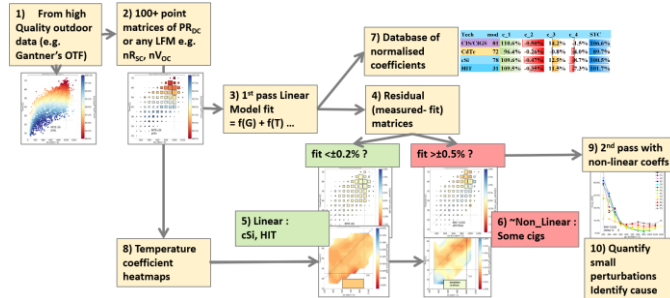


Fig. 16. G_{REF_CELL}/G_{REF_CELL_KG3} vs. clearness index and blue_fraction. Gantner Instruments, Tempe AZ

This graph is also quite smooth and is also used to confirm the spectroradiometer measurements against the ratios of irradiance of the unfiltered and filtered reference cells which is a useful redundancy check when measuring spectrally sensitive modules.

IX. CONCLUSIONS



- High quality outdoor measurements on a variety of PV technologies have been gathered from Gantner's OTF).
- ~100 point Performance matrices have been derived for PR_{DC} or any normalised Loss Factors Model coefficients (e.g. nR_{SC} , nR_{OC} , nV_{OC})
- A linear mechanistic model `mpm_6` was applied to all of the matrices to derive meaningful normalised modelling coefficients.
- Residual values (measured – fitted) have been calculated for all parameters
- Linear modules such as cSi and HIT have been found to have good residual fits, generally $<0.2\%/bin$
- Non-linear modules (some CIGS) might have slightly worse fits $\sim 0.5\%/bin$ that may be monotonic,
- Model fits parameters can be stored in a normalised coefficient database with meaningful coefficients e.g. `c_2` is the temperature coefficient (γ for PR_{DC}) for quick and easy comparison and generation of performance at standard conditions such as STC, LIC etc.
- Temperature coefficient heat maps with 100 points have been generated from the performance matrices and are very uniform for linear devices, some non-uniformity for non-linear devices.
- The non-linear devices found only have small non linearities ($\ll 1\%$) so a second pass can be done on the residuals from a linear fit.
- These perturbations can be identified and quantified with causes such as “high irradiance temperature sensitive Rseries”.
- Optimum analysis comes from the best quality measurements and therefore qualifies as meaningful and trustworthy guidance for large scale power plants.

ACKNOWLEDGMENTS:

Gantner Instruments for providing the data and analysis support.

References

- [IEC 61853 1-4](#)
- [Vogt et al “Interlaboratory Comparison of the PV Module Energy Rating Standard” EUPVSEC Lisbon 2020](#)
- [Mani et al “Power Rating per IEC 61853-1 Standard: A Study Under Natural Sunlight”](#)
- [S. Ransome and J. Sutterlueti “Checking the new IEC 61853.1-4 with high quality 3rd party data to benchmark its practical relevance in energy yield prediction” PVSC-46 Chicago, 2019](#)
- [S. Ransome and J. Sutterlueti “Quantifying long term PV performance and degradation under real outdoor and IEC 61853 test conditions using high quality module IV measurements” 36th EUPVSEC Marseille, 2019](#)
- [PVP/PMC Holmgren, W. C. Hansen and M. Mikofski \(2018\). “pvlib Python: A python package for modeling solar energy systems.” Journal of Open Source Software 3\(29\): 884.](#)